Published in final edited form as:
Am J Physiol Renal Physiol. 2006 December ; 291(6): F1132–F1141. doi:10.1152/ajprenal.00063.2006.

Claudins 6, 9, and 13 are developmentally expressed renal tight junction proteins

Ghazala Abuazza[1], **Amy Becker**[1], **Scott S. Williams**[1], **Sumana Chakravarty**[1], **Hoang-Trang Truong**[1], **Fangming Lin**[1], and **Michel Baum**[1,2]

[1]Department of Pediatrics, University of Texas Southwestern Medical Center at Dallas, Dallas, Texas

[2]Department of Internal Medicine, University of Texas Southwestern Medical Center at Dallas, Dallas, Texas

Abstract

The adult proximal tubule is a low-resistance epithelium where there are high rates of both active transcellular and passive paracellular NaCl transport. We have previously demonstrated that the neonatal rabbit and rat proximal tubule have substantively different passive paracellular transport properties than the adult proximal tubule, which results in a maturational change in the paracellular passive flux of ions. Neonatal proximal tubules have a higher P_{Na}/P_{Cl} ratio and lower chloride and bicarbonate permeabilities than adult proximal tubules. Claudins are a large family of proteins which are the gate keepers of the paracellular pathway, and claudin isoform expression determines the permeability characteristics of the paracellular pathway. Previous studies have shown that claudins 1, 2, 3, 4, 5, 7, 8, 10, 11, 12, 15, and 16 are expressed in the adult mouse kidney. To determine whether there are developmental claudin isoforms, we compared the claudin isoforms present in the neonatal and adult kidney using RT-PCR to detect mRNA of claudin isoforms. Claudin 6, claudin 9, and claudin 13 were either not expressed or barely detectable in the adult mouse kidney using traditional PCR, but were expressed in the neonatal mouse kidney. Using real-time RT-PCR, we were able to detect a low level of claudin 6 mRNA expression in the adult kidney compared with the neonate, but claudin 9 and claudin 13 were only detected in the neonatal kidney. There was the same maturational decrease in these claudin proteins with Western blot analysis. Immunohistochemistry showed high levels of expression of claudin 6 in neonatal proximal tubules, thick ascending limb, distal convoluted tubules, and collecting ducts in a paracellular distribution but there was no expression of claudin 6 in the adult kidney. Using real-time RT-PCR claudin 6 and 9 mRNA were present in 1-day-old proximal convoluted tubules and were virtually undetectable in proximal convoluted tubules from adults. Claudin 13 was not detectable in neonatal or adult proximal convoluted tubules. In summary, we have identified developmentally expressed claudin isoforms, claudin 6, claudin 9, and claudin 13. These paracellular proteins may play a role in the maturational changes in paracellular permeability.

Address for reprint requests and other correspondence: M. Baum, Dept. of Pediatrics, U.T. Southwestern Medical Center, 5323 Harry Hines Blvd., Dallas, TX 75390-9063 (Michel.Baum@UTSouthwestern.edu).

Keywords

renal tubule; renal development; paracellular pathway; neonatal kidney

THE TIGHT JUNCTION DETERMINES the paracellular permeability properties of epithelia (13, 30, 31). The tight junction forms a barrier that separates the apical and basolateral membrane, and the properties of the tight junction proteins determine the permeability of solutes across the paracellular pathway. The tight junction fibrils are composed of occludin and a family of proteins called claudins (16, 17, 29, 49). Many of the components of the tight junction have been identified and characterized (13, 30, 31). Occludin and all members of the claudin family are small proteins, which have 2 extracellular loops, and form a seal at the tight junction between neighboring cells (17, 32). The claudin isoforms present in an epithelium are the major factor determining the permeability properties of the paracellular pathway (2, 11, 12, 15, 31, 44, 45, 48, 53).

The permeability properties vary considerably along the nephron with the proximal tubule having a relatively lower resistance epithelium than the distal nephron (9, 20, 21, 37). Different claudins have been shown to be expressed in different nephron segments (15, 25, 27, 44). The relationship between the claudin isoform present and the permeability properties of the epithelium is best exemplified by the expression of claudin 16 in the thick ascending limb resulting in the high passive divalent cation permeability in this segment (44).

Previous studies have examined the renal expression claudins 1–16 in adult mice (25). The adult kidney was found to express each claudin isoform except claudin 6, 9, 13, and 14 (25). We have previously demonstrated that there is a maturational change in proximal tubule paracellular permeability (35, 37, 42, 43). The purpose of this study was to examine whether there are claudin isoforms expressed in the neonatal kidney that are not expressed in adult kidney.

MATERIALS AND METHODS

Animals

Adult nonpregnant and pregnant C57/B6 mice were obtained from Jackson laboratories. Neonatal kidneys were studied within 24 h of birth. For the in vitro microperfusion studies, mice were studied at 10 –14 days of age. This study conformed to the American Physiological Society's *Guiding Principles in the Care and Use of Laboratory Animals*, and all protocols were approved by the IACUC at the University of Texas Southwestern Medical Center.

Permeability studies

Isolated segments of midcortical and juxtamedullary proximal convoluted tubules (PCT) were perfused as previously described for mice and rabbits (4, 6, 36, 40, 42, 43). Briefly, tubules were dissected in Hanks' balanced salt solution containing (in mM) 137 NaCl, 5 KCl, 0.8 $MgSO_4$, 0.33 Na_2HPO_4, 0.44 KH_2PO_4, 1 $MgCl_2$, 10 Tris hydrochloride, 0.25

$CaCl_2$, 2 glutamine, and 2 L-lactate at 4°C without the use of collagenase. Tubules were transferred to a 1.2 ml temperature-controlled bath. The tubules were perfused using concentric glass pipettes at 38°C.

The relative sodium-to-chloride permeability (P_{Na}/P_{Cl}) and bicarbonate-to-chloride permeabilities (P_{HCO3}/P_{Cl}) in proximal convoluted tubules from mice were determined from the passive transepithelial potential difference (PD) due to imposed ion concentration gradients as previously described in our laboratory and by others (7, 10, 37, 51). The transepithelial PD (in mV) was measured using the perfusion pipette as the bridge into the tubular lumen. All bathing solutions contained 10^{-4} M ouabain to inhibit transepithelial potential difference generated from active transport. Tubules were perfused with an ultrafiltrate-like solution. The compositions of the bathing solutions used to measure dilution potentials are shown in Table 1.

Claudin mRNA expression in neonatal and adult kidney

Renal tissue containing both cortex and medulla (~40 mg) was isolated to determine which claudins were expressed in the neonatal and adult kidney. Total RNA was isolated using a GeneElute Mammalian Total RNA Purification Kit (Sigma, St. Louis, MO). One microgram of total RNA was treated with deoxyribonuclease I to digest genomic DNA according to the manufacturer's instructions (Invitrogen, Carlsbad, CA). cDNA was then prepared using StrataScript Reverse Transcriptase (Stratagene, La Jolla, CA) at an annealing temperature of 25°C for 10 min, extension at 42°C for 50 min, and termination at 70°C for 15 min. The mRNA for specific claudins and GAPDH was amplified using HotStar*Taq* DNA Polymerase (Quiagen, Valencia, CA) with specific primers (Table 2). mRNA was amplified by PCR using a DNA Thermal Cycler (Perkin Elmer, Norwalk, CT). PCR was initiated at 95°C for 15 min followed by 35 cycles of denaturation at 94°C for 45 s, annealing at 55°C for 45 s, and elongation at 72°C for 60 s followed by a final extension at 72°C for 10 min. Negative controls included dissection medium subjected to RT-PCR, and aliquots from samples with reverse transcriptase omitted. The PCR product was separated on a 1% agarose gel containing ethidium bromide in 1× TBE buffer and visualized by UV fluorescence. Verification of claudin 6, claudin 9, and claudin 13 mRNA was performed by direct sequencing of the PCR product. Each experiment was performed at least four times.

Claudin mRNA expression in neonatal and adult proximal convoluted tubules

Kidneys from 1-day-old and adult mice were harvested, sliced in coronal sections, and placed in 10 ml of DMEM (GIBCO, Grand Island, NY) at 37°C containing 1 mg/ml collagenase (Worthington, Lakewood, NJ). The kidney was then vigorously shaken at 37°C for 10 –15 min, ~20 mm of proximal convoluted tubules were dissected free hand and placed in 200 μl of RNA Extraction Buffer, and RNA was isolated using Mini RNA Isolation Kit (Zymed, Orange, CA). c-DNA was prepared using a Cells-to-cDNA II kit (Ambion, Austin, TX) according to the manufacturer's instructions. The mRNA for the claudin isoforms, occludin, and GAPDH was amplified as described above.

Real-time RT-PCR

Real-time RT-PCR was performed using an iCycler PCR thermal cycler (Bio-Rad, Hercules, CA) to determine relative mRNA abundance. Amplification was performed with the primers for claudin 6, claudin 9 and claudin 13 (Table 2) using Syber Green master mix according to the manufacturer's instructions. The cycle where the PCR product exceeded the threshold was noted for claudin 6, claudin 9, claudin 13, and GAPDH and the fold-change was calculated using an exponential function of the difference in thresholds between the various ages (34). Typical tracings are shown in Fig. 3. There was no maturational change in GAPDH expression (not shown). There were 8 experiments in each group. For dissected proximal convoluted tubules the methods were the same as above except that 28S was used as the control which we found preferable in dissected tubule studies. There was no difference in 28S expression in neonates and adults. There were seven experiments in each group.

SDS-PAGE and immunoblotting

Neonatal and adult kidney protein (100 μg/lane) were denatured and separated on a 6% polyacrylamide gel using SDS-PAGE as previously described (5, 41). The proteins were transferred overnight to a polyvinylidene diflouride membrane at 120 –140 mA at 4°C. The blot was blocked with fresh Blotto (5% nonfat milk and 0.1% Tween 20 in PBS, pH 7.4) for 1 h followed by incubation with overnight at 4°C with a primary antibody to mouse claudin 6 (Orbigen, San Diego, CA) at a 1:5,000 dilution, claudin 9 (Aviva Systems Biology, San Diego, CA) at 1:1,000 dilution or claudin 13 (Zymed Laboratories, South San Francisco, CA) at 1:100 dilution.

The blot was then washed extensively with Blotto. The secondary antibody, horseradish peroxidase-conjugated donkey anti-rabbit immunoglobulin, was added at 1:10,000 dilution and incubated at room temperature for 1 h. The blot was again washed with Blotto, and enhanced chemiluminescence was used to detect bound antibody (Amersham Biosciences, Piscataway, NJ). Claudin 6, 9, and 13 protein abundance was quantitated using densitometry. Equal loading of samples was confirmed using an antibody to β-actin at 1:5,000 dilution (Sigma Biochemicals, St. Louis, MO). There were at least six samples in each group.

Immunohistochemistry

The expression of claudin 6 was examined on sections of formalin-fixed and paraffin-embedded neonatal, and adult mouse kidneys. The kidneys were fixed with 10% formalin for 2 h before transfer to 70% ethanol. Kidneys were embedded in paraffin, sectioned at 4-μm thickness, and transferred to glass slides treated with VECTABOND (Vector Laboratories, Burlingame, CA). Kidney sections were deparaffinized with Histoclear (National Diagnostics, Atlanta, GA). Antigen retrieval was performed by boiling the slides in 10 mM Citrate Buffer (pH 6.0) for 20 min in a microwave, followed by Proteinase K treatment (20 μg/ml) for 20 min at room temperature. Sections were blocked with an Avidin/Biotin Blocking Kit (Vector Laboratories) followed by 5% rabbit serum and 1% BSA in PBS for 30 min. Autofluorescence was quenched with 0.1% sodium borohydride in PBS for 30 min at room temperature. Following quenching, sections were incubated with a goat

polyclonal antibody against claudin 6 (Santa Cruz Biotechnology, Santa Cruz, CA) at 1:50 dilution in blocking solution overnight at 4°C. After being washed, sections were incubated with biotinylated anti-goat IgG (Vector Laboratories) at 1:400 for 1 h followed by Rhodamine Avidin D (Vector Laboratories) at 1:400 for 1 h at room temperature. Sections were then costained with nephron specific markers by blocking with 10% goat serum and 1% BSA for 30 min at room temperature followed by incubation with proximal tubular-specific lectin (26), Fluorescein Lotus Lectin (also called *Lotus tetragonobulus* agglutinin or LTA, Vector Laboratories), at a dilution of 1:800; collecting duct-specific lectin (26), Fluorescein *Dolichos Biflorus* Agglutinin (Vector Laboratories), at a dilution of 1:200; thick ascending limb-specific rabbit anti-NKCC-2 antibody (14) at a dilution of 1:400; or distal tubule-specific rabbit anti-thiazide-sensitive NaCl cotransporter antibody, TSC1 (23), at a dilution of 1:400 for 2 h at room temperature. Antibodies to TSC1 and NKCC2 were gifts from Dr. M. Knepper (National Institute of Diabetes and Digestive and Kidney Diseases, National Institutes of Health). After being washed, sections stained with NKCC2 and TSC1 antibodies were incubated with AlexaFluor 488 goat anti-rabbit (Molecular Probes, Eugene, OR) at a dilution of 1:400 for 1 h. Kidney sections were covered with VECTASHIELD with diamidophenylindole (DAPI) to counterstain the nuclei (Vector Laboratories). Fluorescence was visualized with a Zeiss Axioplan 2 epifluorescent microscope (Carl Zeiss Microimaging, Thornwood, NY), and photographs were obtained with a CCD camera. Images were analyzed with Openlab software (Improvision, Lexington, MA). Unfortunately, antibodies to claudin 9 and claudin 13 did not work for immunohistochemistry.

Statistical analysis

Data are reported as means ± SE. ANOVA was used to determine statistical significance if there were more than two groups followed by a post hoc Student-Newman-Keuls if there were more than two groups. An unpaired Student's *t*-test was used for experimental analysis if there were two groups. A P value of <0.05 was considered significant.

RESULTS

Studies showing a maturational difference in permeability of the paracellular pathway have previously been performed in rabbit and the rat (8, 37, 43). To determine whether there was a change in the permeability properties of the paracellular pathway in the mouse, we examined the relative permeability of ions using dilution potentials, a well-described characteristic of the paracellular pathway. There were at least 12 measurements in both groups. As shown in Fig. 1, we found that the P_{Na}/P_{Cl} in proximal convoluted tubules was 1.39 ± 0.23 in neonates (~10 days of age) and 0.89 ± 0.08 in adults, $P < 0.05$. P_{HCO3}/P_{Cl} was 0.16 ± 0.08 in neonates and 0.49 ± 0.09 in adults, $P < 0.05$. Thus there is a maturational decrease in proximal tubule P_{Na}/P_{Cl} and increase in P_{HCO3}/P_{Cl}. This indicates that there is a maturational change in the paracellular pathway in mice as we have previously found in rabbits and rats (8, 37, 43).

Claudin mRNA expression in neonatal and adult kidneys

In the next series of experiments we examined the claudins expressed in neonatal and adult kidneys. As previously described by others using Northern blot analysis (25), we found

claudins 1, 2, 3, 4, 5, 7, 8, 10, 11, 12, 15, and 16 in adult and also in 1-day-old kidneys using PCR. These data are shown in Fig. 2. Unlike previous studies (25, 46), we did detect a faint band for claudin 6 in some adult samples; however, we found greater expression using 1-day-old kidneys. Claudin 9 and claudin 13 were only expressed in neonatal kidneys. The identity of claudin 6, claudin 9, and claudin 13 was confirmed by sequencing. Furthermore, no RT-PCR products for claudin 6, claudin 9, and claudin 13 were detected in samples without the inclusion of reverse transcriptase indicating that no genomic DNA contamination had occurred.

To quantitate the relative abundance of claudin 6, 9, and 13 mRNA expression, we used real-time RT-PCR. There was no difference in GAPDH mRNA during maturation (not shown). However, as shown in Fig. 3, there was an ~100-fold greater claudin 6 expression in 1-day-old neonates than in adults, while claudin 9 and claudin 13 were undetectable in adult kidneys. At 2 wk of age, claudin 6 and claudin 9 mRNA were present but at much lower levels than at 1 day of age. Claudin 13 mRNA was not detectable in kidneys of two wk old mice. There were eight experiments in each group.

Claudin 6, 9, and 13 protein expression in neonatal and adult kidneys

We next examined the relative expression of claudin 6, 9, and 13 protein abundance in 1-day-old, 2-wk-old and adult kidneys using immunoblotting. As shown in Fig. 4, claudin 6 was detected in neonatal, 2-wk-old and adult kidneys. The expression in adult kidneys was far less than in the 1-day-and 2-wk-old mice. Claudin 9 and 13 protein were detected in 1-day-old kidneys and claudin 9 was still detected at 2 wk of age but at a lower level than at 1 day of age. Claudin 13 was virtually undetectable in adult kidneys and barely detectable at 2 wk. There were six experiments in each group. Thus there is a maturational increase in claudin 6, 9, and 13 protein expression during postnatal development.

Immunohistochemical analysis of claudin 6 was combined with staining of nephron-specific markers to localize the expression of claudins at the cellular level. As shown in Fig. 5, claudin 6 expression in the neonatal kidney is clearly detected at apical intercellular junctions of the proximal tubule, thick ascending limb, distal tubule and collecting duct. The level of expression decreased with age. There also appears to be some staining of claudin 6 on the basolateral membrane of the 1-day-old rat in addition to the tight junction. The reason for its localization on the basolateral membrane is unclear but has also been demonstrated for claudin 7 in the distal nephron (27). At 2 wk of age, caludin 6 can only be detected in the proximal tubule and thick ascending limb. Claudin 6 was not visualized by immunostaining in any nephron segment in adult kidney. Antibodies used for Western blot analysis of claudin 9 and claudin 13 did not reveal these proteins by immunohistochemistry in kidney sections. The age-specific and nephron-specific expression of claudin 6 suggests that the expression of claudins is subjected to maturational regulation and may be related to functional changes in ion transport which occur in the postnatal period.

Claudin 6, 9, and 13 protein expression in neonatal and adult proximal convoluted tubules

We next examined the claudins that were expressed in the adult and neonatal proximal convoluted tubule using PCR. In the adult proximal tubule we consistently found claudin 1,

claudin 2, claudin 10a, and claudin 12 expression as shown in Fig. 6. These claudin isoforms were also expressed in neonatal proximal tubules as was claudin 6. Faint bands for claudin 5 and claudin 7 were variably apparent in the neonatal preparation which likely represent contamination with blood vessels from glomeruli and distal tubules, respectively (27, 33). This contamination was likely due to the extreme difficulty of dissecting 1-day-old mouse proximal tubules. Claudin 9 was also variably and minimally expressed in proximal tubules from 1-day-old mice, but we did not detect claudin 13. To determine whether there was a developmental expression of proximal tubules, we performed real time PCR of dissected proximal tubules using primers for claudins 1, 2, 6, 9, 10a, 12, 13 and occludin as shown in Fig. 7. As can be seen, there is no difference in expression of claudins 1, 2, 10a, 12, and occludin between 1-day-old and adult proximal tubules. Claudin 6 mRNA was expressed in proximal convoluted tubules from neonates but was virtually undetectable in adult proximal convoluted tubules. Claudin 9 mRNA was detectable in neonatal tubules but only after ~38 cycles of PCR. Claudin 13 was undetectable in both neonatal and adult proximal convoluted tubules.

DISCUSSION

We have previously demonstrated that neonatal rabbit and rat proximal tubules have different paracellular properties than that of the adult segment. Neonatal rabbit tubules had a lower chloride and bicarbonate permeability, a higher resistance and a higher P_{Na}/P_{Cl} and P_{HCO3}/P_{Cl} than the adult segment (35, 37, 43). We have recently demonstrated developmental changes in the rat proximal tubule perfused in vitro showing that maturational changes in proximal tubule permeability are not limited to the rabbit (8). While direct measurement of ion permeability is not technically possible in neonatal mice, we were able to measure P_{Na}/P_{Cl} and P_{HCO3}/P_{Cl} and found developmental proximal tubule changes between ~10-day-old and adult mice as we have previously described in rabbits and rats (7, 35, 37, 43). Interestingly, the P_{Na}/P_{Cl} was higher in the neonate than adult rabbit proximal straight tubule, rat proximal convoluted tubule (but not straight tubule) and in mouse proximal convoluted tubules. The P_{HCO3}/P_{Cl} was lower in the mouse neonatal proximal convoluted tubule than in the adult, which is the opposite of that in the rabbit proximal straight tubule. There was no developmental difference in the rat proximal straight and convoluted tubule P_{HCO3}/P_{Cl} (37). Thus, while there are some species differences there is a maturational change in this paracellular property in all species examined.

There are many ways in which the permeability properties of the nephron can affect transport. This is exemplified by the proximal tubule which receives the glomerular filtrate and within 1 mm there are substantive changes in composition of the luminal fluid which can affect passive transport (28, 38). There is preferential reabsorption of organic solutes in the early proximal tubule which are reabsorbed by sodium-dependent mechanisms generating a lumen negative transepithelial potential difference. This provides a driving force for the paracellular transport of anions such as chloride, or the negative potential difference can be a driving force for the paracellular diffusion of cations from the blood into the tubular lumen. The fraction of sodium secretion to chloride absorption due to this potential difference is entirely dependent on P_{Na}/P_{Cl}. Bicarbonate is also preferentially reabsorbed over chloride ions which leaves the luminal fluid with a higher chloride

concentration and lower bicarbonate concentration than the peritubular fluid (28, 38). The relative amount of chloride absorption to bicarbonate secretion across the paracellular pathway is dependent on the P_{HCO3}/P_{Cl}. In the mouse there is a maturational change in both the P_{Na}/P_{Cl} and P_{HCO3}/P_{Cl} which can affect passive paracellular NaCl transport.

The cause for the maturational change in paracellular permeability is unclear at present. We have previously shown that claudin 2 protein expression is fourfold greater in neonatal proximal tubules than in adult proximal tubules while occludin protein abundance increases during postnatal development using immunoblot analysis and immunohistochemistry in the rat (18). Claudin 2 has been shown to increase the permeability of sodium, and the high paracellular sodium-to-chloride permeability in neonates compared with adults may be explained by the high level of expression of this claudin (50).

A previous study by Reyes et al. (39) has examined the maturation of claudin 1– 8 expression in the rabbit. They found that claudin 1, 2, 3, 4, 7, 8 were present in dissected proximal tubules of adults. Neonatal proximal tubules expressed claudins 1– 4 but not claudin 7 and 8. The difference between the studies by Reyes et al. and this one may be due to a species difference or the fact that they performed two rounds of PCR, which may have detected expression of very low levels of mRNA or potentially resulted in erroneous amplification.

In the present study we found no difference in claudin 1, 2, 10a, 12 or occludin mRNA in 1-day-old neonatal and adult proximal convoluted tubules using real time RT-PCR. Claudin 6 was expressed in dissected neonatal proximal convoluted tubules and may play a role in the developmental changes in paracellular permeability in this segment. Claudin 6 has two aspartic acid moieties in the first extracellular loop at amino acids 68 and 76 which theoretically would impede anion permeability as we have found in the rat and rabbit (35, 37, 42, 43). Claudin 9 was only consistently detectable in proximal convoluted tubules of 1-day-old neonates and only after more than 35 cycles of amplification. Claudin 13 was not detectable. It is possible that claudin 9 and 13 play a role in determining neonatal paracellular permeability in a distal nephron segment.

Claudin 6 was first identified from EST sequences from embryos by Morita et al. (32). However, when this group tried to identify the expression of claudin 6 mRNA using Northern blot analysis of adult tissues, they failed to detect expression in any tissue examined in spite of the fact that they found tissue specific expression of several other claudins (32). They hypothesized that claudin 6 may be regulated developmentally. Our data are consistent with this hypothesis. Claudin 6 was also independently cloned from mouse embryoid bodies using differential display (46). Claudin 6 was not present in mesen-chymal cells and was only expressed in embryonic cells committed to an epithelial fate (46). The protein expression of claudin 6 increased in embryoid bodies in parallel with the expression of keratin 8 and the formation of the epithelial zone. Overexpression of claudin 6 in mice results in an increase in expression in its normal suprabasal epithelial layer, formation of a defective epithelial permeability barrier and death within 48 h from increased water loss though the skin (47).

Claudin 6 may be developmentally expressed in other tissues. Claudin 6 was found in *E14* and *E16* mouse submandibular ducts but was absent postnatally (19). Unlike the above findings in the submandibular duct, claudin 6 is expressed postnatally in the kidney, although there is decline with post-natal maturation. This may be due to the fact that the postnatal kidney in the mouse is not fully developed and that nephro-genesis is still occurring until for ~10 days postnatally.

Less is known about the expression and function of claudin 9 and claudin 13 than claudin 6. Claudin 9 mRNA has been found using RT-PCR in human corneal epithelial cells (3, 52), and claudin 9 protein has been demonstrated in mouse inner ear and intestine (22, 24). Claudin 13 mRNA has been localized to the adult mouse bladder and intestine (1, 22).

In the present study, claudin 6 was present in each nephron segment studied. While only the permeability properties of the proximal tubule have been studied in development, the presence of claudin 6 in other segments suggests that this developmental claudin may affect the permeability properties in other nephron segments. Unfortunately, our antibodies for claudin 9 and claudin 13 did not work for immunohistochemistry and the nephron distribution for these claudins is unclear at present. How claudin -6, 9, and 13 affect paracellular permeability and its role in postnatal electrolyte homeostasis remain to be determined.

Acknowledgments

We thank Dr. R. Quigley for reviewing this manuscript.

GRANTS

This work was supported by National Institutes of Health Grant DK-41612.

References

1. Acharya P, Beckel J, Ruiz WG, Wang E, Rojas R, Birder L, Apodaca G. Distribution of the tight junction proteins ZO-1, occludin, and claudin-4, -8, and -12 in bladder epithelium. Am J Physiol Renal Physiol. 2004; 287:F305–F318. [PubMed: 15068973]
2. Balda MS, Flores-Maldonado C, Cereijido M, Matter K. Multiple domains of occludin are involved in the regulation of paracellular permeability. J Cell Biochem. 2000; 78:85–96. [PubMed: 10797568]
3. Ban Y, Dota A, Cooper LJ, Fullwood NJ, Nakamura T, Tsuzuki M, Mochida C, Kinoshita S. Tight junction-related protein expression and distribution in human corneal epithelium. Exp Eye Res. 2003; 76:663–669. [PubMed: 12742348]
4. Baum M, Berry CA. Evidence for neutral transcellular NaCl transport and neutral basolateral chloride exit in the rabbit convoluted tubule. J Clin Invest. 1984; 74:205–211. [PubMed: 6736248]
5. Baum M, Biemesderfer D, Gentry D, Aronson PS. Ontogeny of rabbit renal cortical NHE3 and NHE1: effect of glucocorticoids. Am J Physiol Renal Fluid Electrolyte Physiol. 1995; 268:F815–F820.
6. Baum M, Loleh S, Saini N, Seikaly M, Dwarakanath V, Quigley R. Correction of proximal tubule phosphate transport defect in Hyp mice in vivo and in vitro with indomethacin. Proc Natl Acad Sci USA. 2003; 100:11098–11103. [PubMed: 12953100]
7. Baum M, Quigley R. Thyroid hormone modulates rabbit proximal straight tubule paracellular permeability. Am J Physiol Renal Physiol. 2004; 286:F477–F482. [PubMed: 14644749]

8. Baum M, Quigley R. Maturation of rat proximal tubule chloride permeability. Am J Physiol Regul Integr Comp Physiol. 2005; 289:R1659–R1664. [PubMed: 16051720]
9. Berry CA. Lack of effect of peritubular protein on passive NaCl transport in the rabbit proximal tubule. J Clin Invest. 1983; 71:268–281. [PubMed: 6822664]
10. Berry CA, Rector FC Jr. Relative sodium-to-chloride permeability in the proximal convoluted tubule. Am J Physiol Renal Fluid Electrolyte Physiol. 1978; 235:F592–F604.
11. Colegio OR, Itallie CV, Rahner C, Anderson JM. Claudin extra-cellular domains determine paracellular charge selectivity and resistance but not tight junction fibril architecture. Am J Physiol Cell Physiol. 2003; 284:C1346–C1354. [PubMed: 12700140]
12. Colegio OR, Van Itallie CM, McCrea HJ, Rahner C, Anderson JM. Claudins create charge-selective channels in the paracellular pathway between epithelial cells. Am J Physiol Cell Physiol. 2002; 283:C142–C147. [PubMed: 12055082]
13. Denker BM, Nigam SK. Molecular structure and assembly of the tight junction. Am J Physiol Renal Physiol. 1998; 274:F1–F9.
14. Ecelbarger CA, Terris J, Hoyer JR, Nielsen S, Wade JB, Knepper MA. Localization and regulation of the rat renal Na^+-K^+-$2Cl^-$ cotrans-porter, BSC-1. Am J Physiol Renal Fluid Electrolyte Physiol. 1996; 271:F619–F628.
15. Enck AH, Berger UV, Yu AS. Claudin-2 is selectively expressed in proximal nephron in mouse kidney. Am J Physiol Renal Physiol. 2001; 281:F966–F974. [PubMed: 11592954]
16. Furuse M, Fujita K, Hiiragi T, Fujimoto K, Tsukita S. Claudin-1 and -2: novel integral membrane proteins localizing at tight junctions with no sequence similarity to occludin. J Cell Biol. 1998; 141:1539–1550. [PubMed: 9647647]
17. Furuse M, Hirase T, Itoh M, Nagafuchi A, Yonemura S, Tsukita S, Tsukita S. Occludin: a novel integral membrane protein localizing at tight junctions. J Cell Biol. 1993; 123:1777–1788. [PubMed: 8276896]
18. Haddad M, Lin F, Dwarakanath V, Cordes K, Baum M. Developmental changes in proximal tubule tight junction proteins. Pediatr Res. 2005; 57:453–457. [PubMed: 15585672]
19. Hashizume A, Ueno T, Furuse M, Tsukita S, Nakanishi Y, Hieda Y. Expression patterns of claudin family of tight junction membrane proteins in developing mouse submandibular gland. Dev Dyn. 2004; 231:425–431. [PubMed: 15366020]
20. Helman SI. Determination of electrical resistance of the isolated cortical collecting tubule and its possible anatomical location. Yale J Biol Med. 1972; 45:339–345. [PubMed: 4638656]
21. Helman SI, Grantham JJ, Burg MB. Effect of vasopressin on electrical resistance of renal cortical collecting tubules. Am J Physiol. 1971; 220:1825–1832. [PubMed: 5087832]
22. Holmes JL, Van Itallie CM, Rasmussen JE, Anderson JM. Claudin profiling in the mouse during postnatal intestinal development and along the gastrointestinal tract reveals complex expression patterns. Gene Expr Patterns. In press.
23. Kim GH, Masilamani S, Turner R, Mitchell C, Wade JB, Knep-per MA. The thiazide-sensitive Na-Cl cotransporter is an aldosterone-induced protein. Proc Natl Acad Sci USA. 1998; 95:14552–14557. [PubMed: 9826738]
24. Kitajiri SI, Furuse M, Morita K, Saishin-Kiuchi Y, Kido H, Ito J, Tsukita S. Expression patterns of claudins, tight junction adhesion molecules, in the inner ear. Hear Res. 2004; 187:25–34. [PubMed: 14698084]
25. Kiuchi-Saishin Y, Gotoh S, Furuse M, Takasuga A, Tano Y, Tsukita S. Differential expression patterns of claudins, tight junction membrane proteins, in mouse nephron segments. J Am Soc Nephrol. 2002; 13:875–886. [PubMed: 11912246]
26. Laitinen L, Virtanen I, Saxen L. Changes in the glycosylation pattern during embryonic development of mouse kidney as revealed with lectin conjugates. J Histochem Cytochem. 1987; 35:55–65. [PubMed: 3794309]
27. Li WY, Huey CL, Yu AS. Expression of claudin-7 and -8 along the mouse nephron. Am J Physiol Renal Physiol. 2004; 286:F1063–F1071. [PubMed: 14722018]
28. Liu FY, Cogan MG. Axial heterogeneity in the rat proximal convoluted tubule. I. Bicarbonate, chloride, and water transport. Am J Physiol Renal Fluid Electrolyte Physiol. 1984; 247:F816–F821.

29. McCarthy KM, Skare IB, Stankewich MC, Furuse M, Tsukita S, Rogers RA, Lynch RD, Schneeberger EE. Occludin is a functional component of the tight junction. J Cell Sci. 1996; 109:2287–2298. [PubMed: 8886979]
30. Mitic LL, Anderson JM. Molecular architecture of tight junctions. Annu Rev Physiol. 1998; 60:121–142. [PubMed: 9558457]
31. Mitic LL, Van Itallie CM, Anderson JM. Molecular physiology and pathophysiology of tight junctions I. Tight junction structure and function: lessons from mutant animals and proteins. Am J Physiol Gastrointest Liver Physiol. 2000; 279:G250–G254. [PubMed: 10915631]
32. Morita K, Furuse M, Fujimoto K, Tsukita S. Claudin multigene family encoding four-transmembrane domain protein components of tight junction strands. Proc Natl Acad Sci USA. 1999; 96:511–516. [PubMed: 9892664]
33. Morita K, Sasaki H, Furuse M, Tsukita S. Endothelial claudin: claudin-5/TMVCF constitutes tight junction strands in endothelial cells. J Cell Biol. 1999; 147:185–194. [PubMed: 10508865]
34. Pfaffl MW. A new mathematical model for relative quantification in real-time RT-PCR. Nucleic Acids Res. 2001; 29:e45. [PubMed: 11328886]
35. Quigley R, Baum M. Developmental changes in rabbit juxtamedullary proximal convoluted tubule bicarbonate permeability. Pediatr Res. 1990; 28:663–666. [PubMed: 2178241]
36. Quigley R, Baum M. Effects of epidermal growth factor and transforming growth factor-alpha on rabbit proximal tubule solute transport. Am J Physiol Renal Fluid Electrolyte Physiol. 1994; 266:F459–F465.
37. Quigley R, Baum M. Developmental changes in rabbit proximal straight tubule paracellular permeability. Am J Physiol Renal Physiol. 2002; 283:F525–F531. [PubMed: 12167604]
38. Rector FC Jr. Sodium, bicarbonate, and chloride absorption by the proximal tubule. Am J Physiol Renal Fluid Electrolyte Physiol. 1983; 244:F461–F471.
39. Reyes JL, Lamas M, Martin D, del Carmen NM, Islas S, Luna J, Tauc M, Gonzalez-Mariscal L. The renal segmental distribution of claudins changes with development. Kidney Int. 2002; 62:476–487. [PubMed: 12110008]
40. Salmon RF, Baum M. Intracellular cystine loading inhibits transport in the rabbit proximal convoluted tubule. J Clin Invest. 1990; 85:340–344. [PubMed: 2298908]
41. Shah M, Gupta N, Dwarakanath V, Moe OW, Baum M. Ontogeny of Na^+/H^+ antiporter activity in rat proximal convoluted tubules. Pediatr Res. 2000; 48:206–210. [PubMed: 10926296]
42. Shah M, Quigley R, Baum M. Maturation of proximal straight tubule NaCl transport: role of thyroid hormone. Am J Physiol Renal Physiol. 2000; 278:F596–F602. [PubMed: 10751220]
43. Sheu JN, Baum M, Bajaj G, Quigley R. Maturation of rabbit proximal convoluted tubule chloride permeability. Pediatr Res. 1996; 39:308–312. [PubMed: 8825805]
44. Simon DB, Lu Y, Choate KA, Velazquez H, Al Sabban E, Praga M, Casari G, Bettinelli A, Colussi G, Rodriguez-Soriano J, McCredie D, Milford D, Sanjad S, Lifton RP. Paracellin-1, a renal tight junction protein required for paracellular Mg^{2+} resorption. Science. 1999; 285:103–106. [PubMed: 10390358]
45. Tsukita S, Furuse M. Pores in the wall: claudins constitute tight junction strands containing aqueous pores. J Cell Biol. 2000; 149:13–16. [PubMed: 10747082]
46. Turksen K, Troy TC. Claudin-6: a novel tight junction molecule is developmentally regulated in mouse embryonic epithelium. Dev Dyn. 2001; 222:292–300. [PubMed: 11668606]
47. Turksen K, Troy TC. Permeability barrier dysfunction in transgenic mice overexpressing claudin 6. Development. 2002; 129:1775–1784. [PubMed: 11923212]
48. Van Itallie C, Rahner C, Anderson JM. Regulated expression of claudin-4 decreases paracellular conductance through a selective decrease in sodium permeability. J Clin Invest. 2001; 107:1319–1327. [PubMed: 11375422]
49. Van Itallie CM, Anderson JM. The molecular physiology of tight junction pores. Physiology. 2004; 19:331–338. [PubMed: 15546850]
50. Van Itallie CM, Fanning AS, Anderson JM. Reversal of charge selectivity in cation or anion-selective epithelial lines by expression of different claudins. Am J Physiol Renal Physiol. 2003; 285:F1078–F1084. [PubMed: 13129853]

51. Warnock DG, Yee VJ. Anion permeabilities of the isolated perfused rabbit proximal tubule. Am J Physiol Renal Fluid Electrolyte Physiol. 1982; 242:F395–F405.

52. Yi X, Wang Y, Yu FS. Corneal epithelial tight junctions and their response to lipopolysaccharide challenge. Invest Ophthalmol Vis Sci. 2000; 41:4093–4100. [PubMed: 11095601]

53. Yu AS, Enck AH, Lencer WI, Schneeberger EE. Claudin-8 expression in Madin-Darby canine kidney cells augments the paracellular barrier to cation permeation. J Biol Chem. 2003; 278:17350–17359. [PubMed: 12615928]

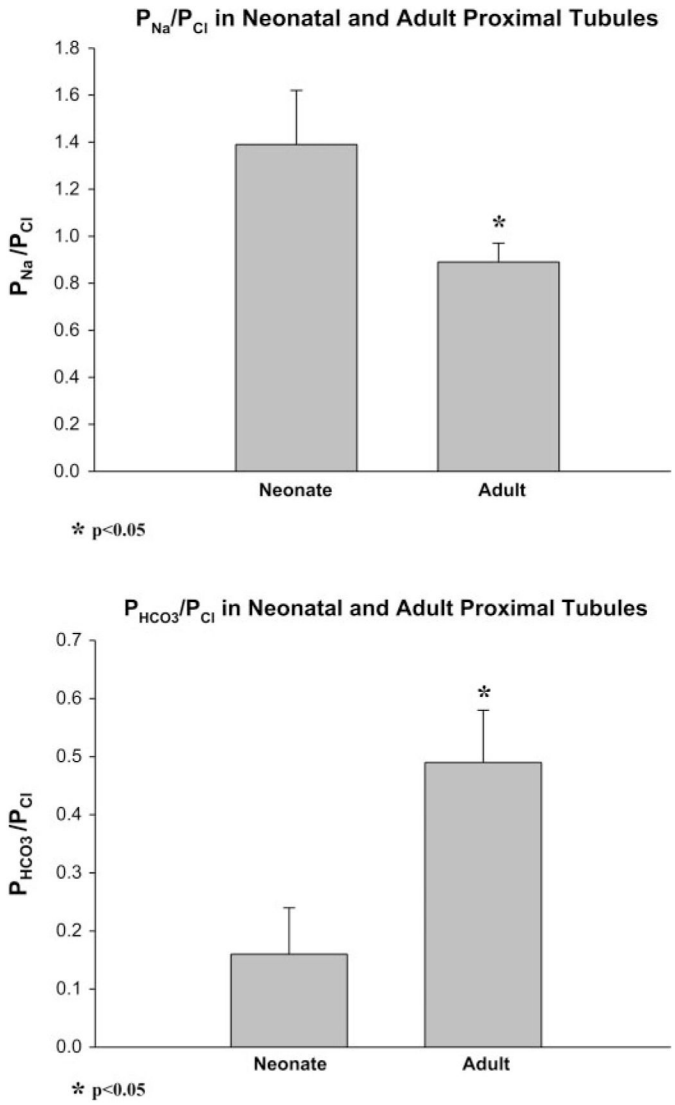

Fig. 1.

$P_{Na/PCl}$ and P_{HCO3}/P_{Cl} in neonatal (~10 days) and adult mouse proximal tubules where *P* is permeability. $P_{Na/PCl}$ and P_{HCO3}/P_{Cl} were measured using dilution potentials in the absence of active transport. There is a maturational change in both consistent with a maturational difference in the paracellular pathway during development in the mouse proximal tubule.

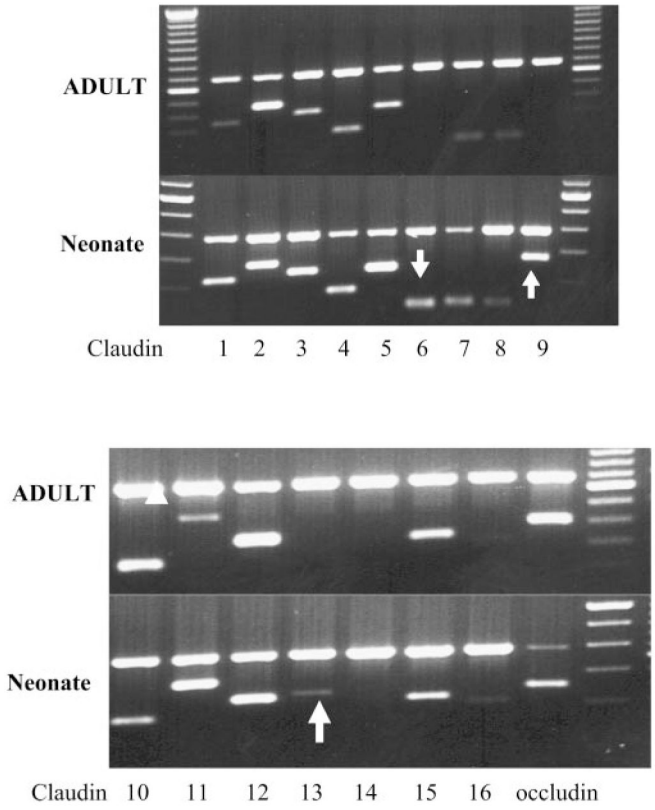

Fig. 2.

Gel showing PCR product for claudin 1–16 in 1-day-old neonates and adults. Arrows denote the presence of claudin 6, claudin 9, and claudin 13 in the neonate. Note that there is no detectable claudin 6, claudin 9, and claudin 13 band in the adult samples. *Top* band is GAPDH.

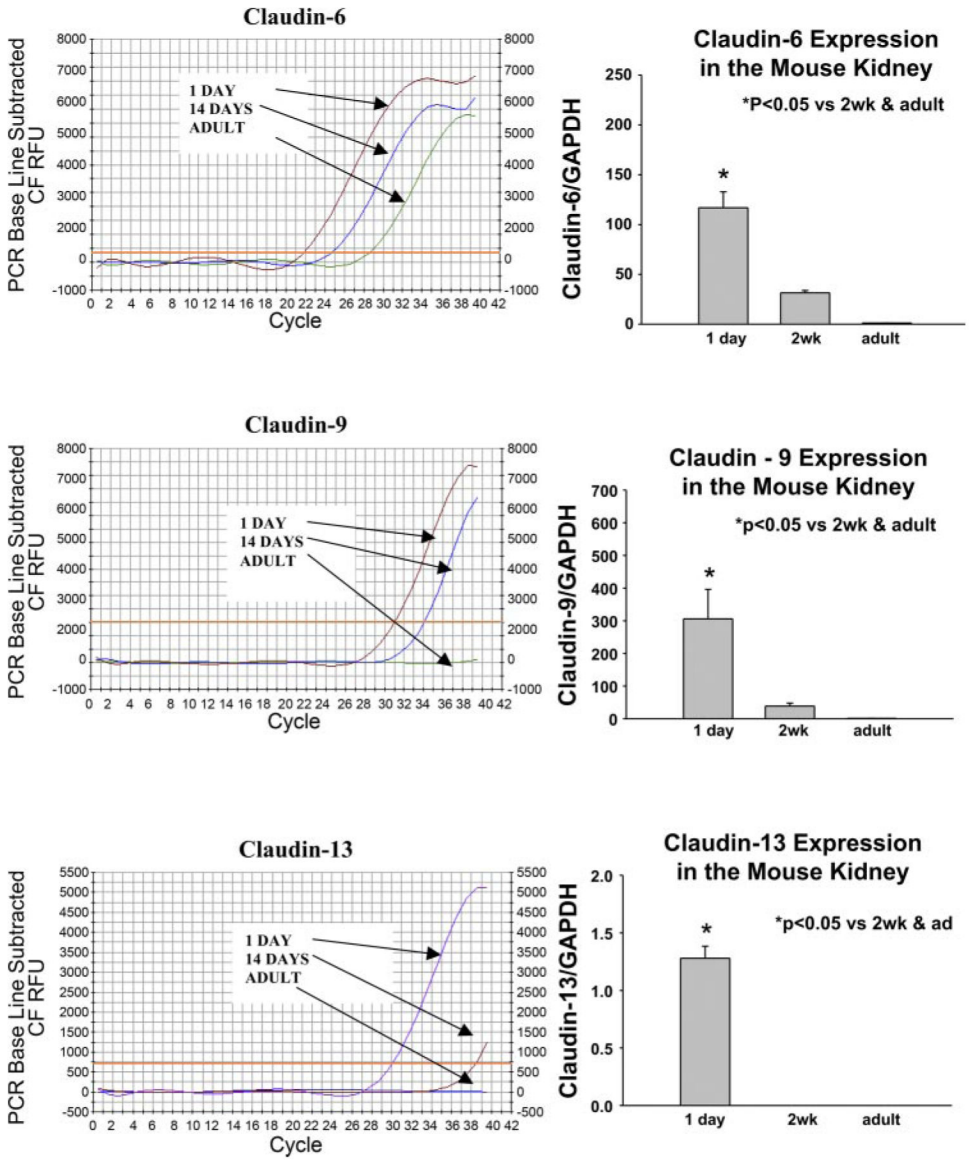

Fig. 3.

PCR profile for claudin 6, 9, 13 in 1-day-old, 2-wk-old, and adult mice kidney using quantitative real-time RT-PCR. To the *right* of each profile is a summary of experiments showing a developmental decrease in mRNA expression. This difference in these claudin isoforms was significant showing a maturational change during postnatal development.

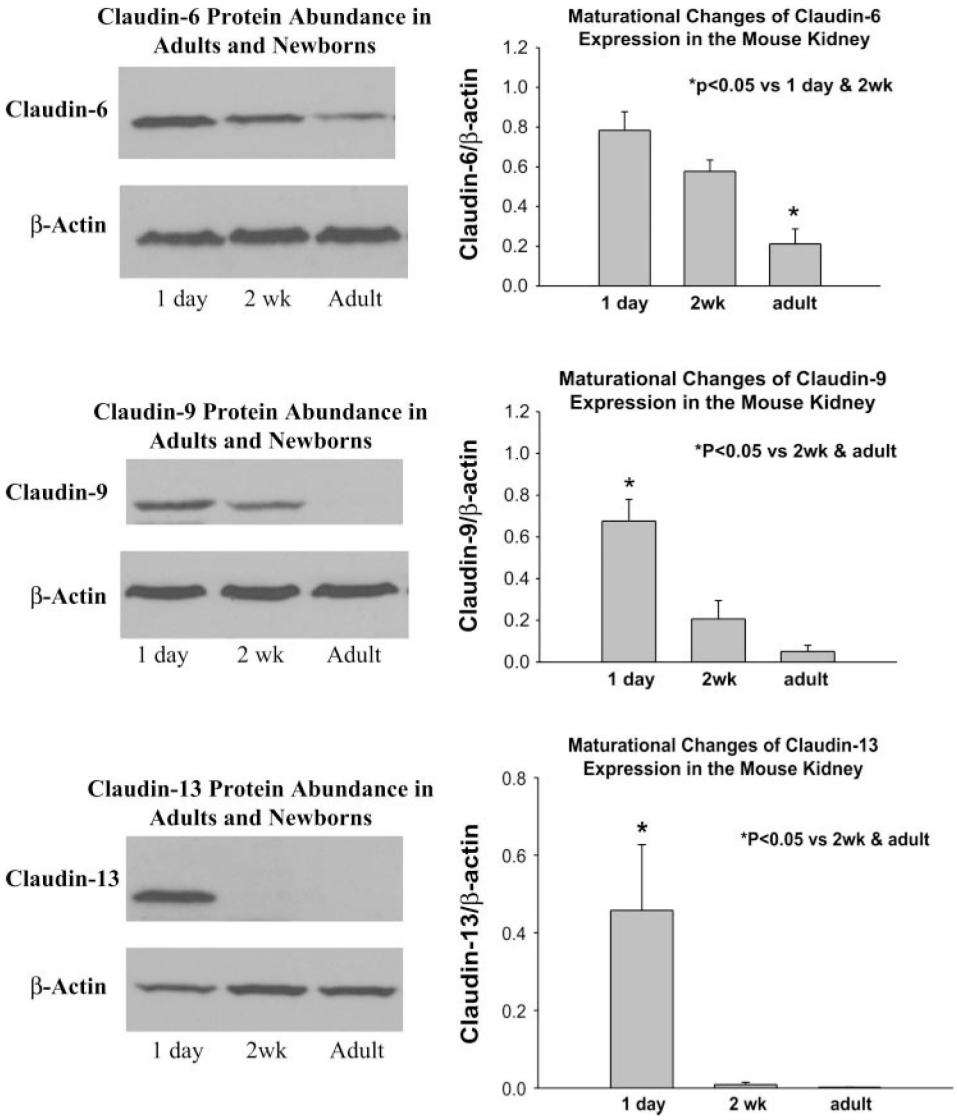

Fig. 4.

Immunoblots showing claudin claudin 6, 9, 13 expression in 1-day-old, 2-wk-old, and adult kidney. β-Actin is below showing equal loading. Also shown is the result of densitometry showing that there is a developmental decrease in expression of these claudin isoforms.

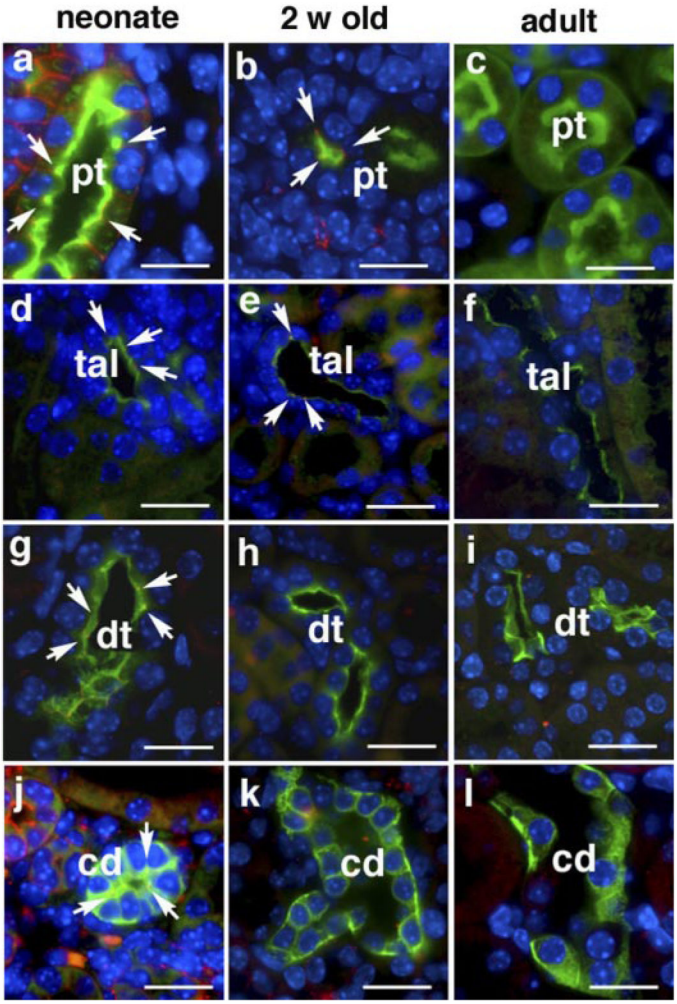

Fig. 5.

Expression of claudin 6 in the kidneys of neonatal, 2-wk-old, and adult mice. Kidney sections were costained with anti-claudin 6 antibody (red) and markers of nephron segments (green). Tubular markers used were LTA for proximal tubules (pt), NKCC2 for thick ascending limb (tal), TSC for distal tubules (dt), and DBA for collecting duct (cd). Note the expression of claudin 6 at the apical aspect of the intercellular junction (arrows) in all the above nephron segments in neonatal kidneys (*a*, *d*, *g*, and *j*). In 2-wk-old mouse kidneys, claudin 6 was detected in proximal tubules (*b*) and in thick ascending limbs (*e*), but not in distal tubules (*h*) and collecting duct (*k*). In adult kidneys, claudin 6 expression was not detected by immunostaining (*c*, *f*, *i*, and *l*). Nuclei were counterstained with DAPI and images were merged. Scale bar = 20 μm.

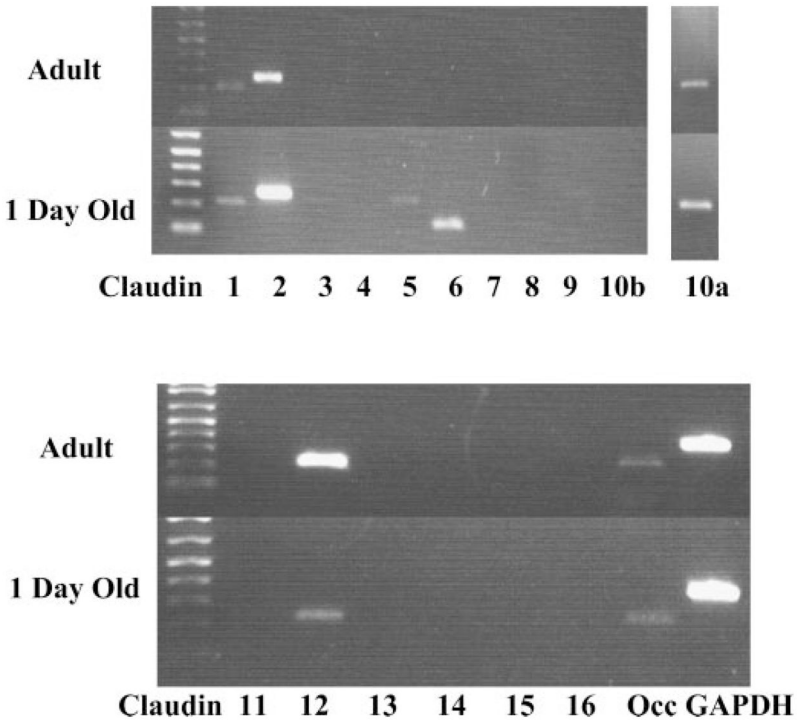

Fig. 6.

Gel showing PCR product for claudin 1–16 in 1-day-old neonatal and adult-dissected proximal convoluted tubules. Arrow denotes the presence of claudin 6 in the neonate. Note that there is no detectable claudin 6 in the adult. Claudin 5 in the neonate is likely contaminant from glomerular vessels (33). A faint band for claudin 9 was sometimes found. Claudin 10b splice variant was not detected, but the claudin 10a splice variant was detected in adult and neonatal proximal tubules. The band for claudin 10a was run on a separate gel, and the image was merged on this figure.

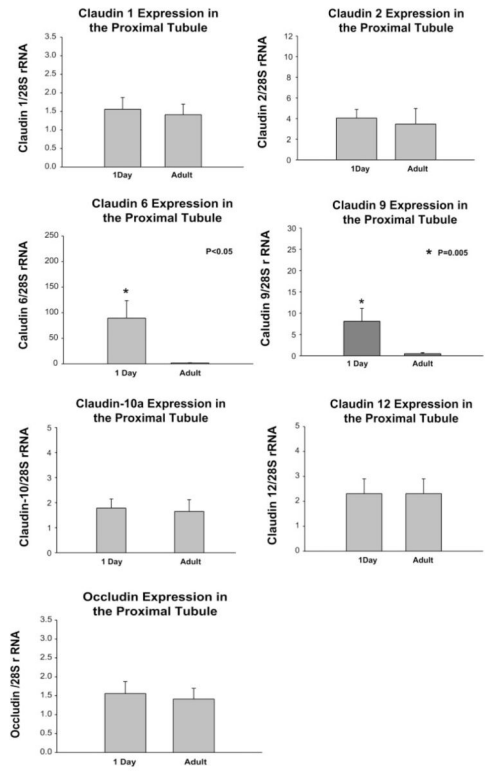

Fig. 7.

PCR profile for claudin 1, 2, 6, 9, 10a, 12 and occludin in 1-day-old and adult mice proximal convoluted tubules (PCT) using quantitative real-time RT-PCR. Shown is a summary of 6 experiments with ~20 mm of PCT demonstrating comparable claudin 1, 2, 10a, 12 and occludin mRNA expression in 1-day-old and adult PCT. Claudin 6 and claudin 9 were detectable in 1-day-old tubules but virtually undetectable in adult PCT. This difference in these claudin isoforms was significant showing a maturational change during postnatal development. Claudin 13 was not detected in 1-day-old or adults.

Table 1

Solutions used to measure P_{Na}/P_{Cl} and P_{HCO3}/P_{Cl}

	Ultrafiltrate-like Solution, mM	NaCl Dilution, mM	$NaHCO_3$ Dilution, mM
NaCl	104	54	104
$NaHCO_3$	25	25	5
Na_2HPO_4	4	4	4
NaAc	7.5	7.5	7.5
$CaCl_2$	1	1	1
$MgSO_4$	1	1	1
KCl	5	5	5
Glucose	5	5	5
Alanine	5	5	5
Urea	5	5	5
Mannitol		*	*

*Mannitol was added to increase the osmolality to 295 mosmol/kgH_2O. *P*, permeability.

Table 2

Primers for PCR of claudins

Primers	Type	Sequence	Exon Location
Claudin 1-555	F	TTA GTG GCC ACA GCA TGG TA	Exon 3
Claudin 1-769	R	GAA GGT GTT GGC TTG GGA TA	Exon 4
Claudin 2-150	F	TAT GTT GGT GCC AGC ATT GT	Exon 2
Claudin 2-415	R	ACT CCA CCC ACT ACA GCC AC	
Claudin 3-466	F	GAG ATG GGA GCT GGG TTG TA	Exon 1
Claudin 3-696	R	TGC TGG TAG TGG TGA CGG TA	
Claudin 4-172	F	AGC ACA GGT CAG ATG CAG TG	Exon 1
Claudin 4-335	R	GTC TCG TCC TCC ATG CAG TG	
Claudin 5-944	F	GCT CTC AGA GTC CGT TGA CC	Exon 1
Claudin 5-1178	R	CTG CCC TTT CAG GTT AGC AG	
Claudin 6-29	F	GCA GTC TCT TTT GCA GGC TC	Exon 1
Claudin 6-153	R	CCC AAG ATT TGC AGA CCA GT	Exon 3
Claudin 7-405	F	AGC ATG TTC CTG GAT TGG TC	Exon 3
Claudin 7-532	R	CCA GAA GGA CCA GAG CAG AC	Exon 4
Claudin 8-190	F	TGC AAG GTC TAC GAC TCC CT	Exon 1
Claudin 8-314	R	GTG CAC TTC ATT CCG AGG AT	
Claudin 9-179	F	GCC AGA TGC AGT GCA AAG TA	Exon 1
Claudin 9-442	R	AAA AAT CCT GGA TGA TGG CA	
Claudin 10a-20	F	TTG TCA GGT CTG TGT TCC ATG ACA GG	Exon 4
Claudin 10a-220	R	CAT TCT GGG TGT CTT GTT GTT GTC GG	Exon 5/6
Claudin 10b-163	F	ATC TGC GTT ACC GAT TCC AC	Exon 2
Claudin 10b-340	R	GAT CTG AGC CTC CGA CTT TG	Exon 3
Claudin 11-361	F	CTG GTG GAC ATC CTC ATC CT	Exon 1
Claudin 11-644	R	CAA CCT GCG TAC AGC GAG TA	Exon 3
Claudin 12-226	F	GAC AGG CTG CTT GGA GAA AC	Exon 4
Claudin 12-450	R	CCC GTG TAA ATC GTC AGG TT	Exon 5
Claudin 13-634	F	TCT TTA ACC CAT TGC TTG GC	Exon 1
Claudin 13-870	R	AGG AAG TTT TCC CCT CCA GA	Exon 2
Claudin 14-356	F	AAG ACT GTT GAA GCC GCA GT	Exon 2
Claudin 14-567	R	AGG AAG CCT AGG AGC TGG AC	Exon 3
Claudin 15-723	F	CTC TAC TTG GGC TGG AGT GC	Exon 4
Claudin 15-937	R	CAG GCC AGA GCT TCC TAC AC	Exon 5
Claudin 16-566	F	TTT ACG TCG AAC GCT CCT CT	Exon 4
Claudin 16-765	R	TGA ATA GGG CTT CCT CAT GG	Exon 5

F, forward; R, reverse.